

# Neuroprotective effect of melatonin in experimental optic neuritis in rats

**Abstract:** Optic neuritis (ON) is an inflammatory, demyelinating, and neurodegenerative condition of the optic nerve, which might induce permanent vision loss. Currently, there are no effective therapies for this disorder. We have developed an experimental model of primary ON in rats through a single microinjection of 4.5  $\mu\text{g}$  of bacterial lipopolysaccharide (LPS) into the optic nerve. Since melatonin acts as a pleiotropic therapeutic agent in various neurodegenerative diseases, we analyzed the effect of melatonin on LPS-induced ON. For this purpose, LPS or vehicle were injected into the optic nerve from adult male *Wistar* rats. One group of animals received a subcutaneous pellet of 20 mg melatonin at 24 hr before vehicle or LPS injection, and another group was submitted to a sham procedure. Melatonin completely prevented the decrease in visual evoked potentials (VEPs), and pupil light reflex (PLR), and preserved anterograde transport of cholera toxin  $\beta$ -subunit from the retina to the superior colliculus. Moreover, melatonin prevented microglial reactivity (ED1-immunoreactivity,  $P < 0.01$ ), astrocytosis (glial fibrillary acid protein-immunostaining,  $P < 0.05$ ), demyelination (luxol fast blue staining,  $P < 0.01$ ), and axon (toluidine blue staining,  $P < 0.01$ ) and retinal ganglion cell (Brn3a-immunoreactivity,  $P < 0.01$ ) loss, induced by LPS. Melatonin completely prevented the increase in nitric oxide synthase 2, cyclooxygenase-2 levels (Western blot) and TNF $\alpha$  levels, and partly prevented lipid peroxidation induced by experimental ON. When the pellet of melatonin was implanted at 4 days postinjection of LPS, it completely reversed the decrease in VEPs and PLR. These data suggest that melatonin could be a promising candidate for ON treatment.

**Marcos L. Aranda<sup>1</sup>,  
María F. González Fleitas<sup>1</sup>,  
Andrea De Laurentiis<sup>2</sup>,  
María I. Keller Sarmiento<sup>1</sup>,  
Mónica Chianelli<sup>1</sup>,  
Pablo H. Sande<sup>1</sup>,  
Damián Dorfman<sup>1</sup> and  
Ruth E. Rosenstein<sup>1</sup>**

<sup>1</sup>Laboratory of Retinal Neurochemistry and Experimental Ophthalmology, Department of Human Biochemistry, School of Medicine/CEFyBO, University of Buenos Aires/CONICET, Buenos Aires, Argentina; <sup>2</sup>CEFyBO, CONICET, Buenos Aires, Argentina

**Key words:** axoglial alterations, melatonin, optic neuritis, pupil light reflex, retinal ganglion cells, visual evoked potentials

Address reprint requests to Dr. Ruth E. Rosenstein, Departamento de Bioquímica Humana, Facultad de Medicina/CEFyBO, Universidad de Buenos Aires/CONICET, Paraguay 2155, 5°P, (1121), Buenos Aires, Argentina.  
E-mail: ruthr@fmed.uba.ar

Received December 1, 2016;  
Accepted February 9, 2016.

## Introduction

Optic neuritis (ON), the most common optic neuropathy affecting young adults, is a condition involving primary inflammation, demyelination, and axonal injury of the optic nerve, which leads to visual dysfunction and retinal ganglion cell (RGC) loss (reviewed by [1] and [2]). The annual incidence of ON is approximately 5 in 100,000, with a prevalence estimated to be 115 in 100,000 [3]. Clinical features of ON include peri- or retro-ocular pain accentuated by eye movement, abnormal visual acuity and field, distorted color vision, afferent pupillary defect, and abnormal visual evoked potentials (VEPs) [1, 2]. ON manifests as acute and severe decreased vision for 1–2 wks, then self-recovers over 1–3 months in most of the patients; however, varying degree of permanent visual dysfunction can occur in ~50% of patients. Even if visual acuity improves, most patients have some residual visual function deficits, such as disturbances of contrast sensitivity, color vision, visual field, stereopsis, pupillary reaction, and VEPs [1, 2]. Moreover, repeated episodes of ON can result in optic nerve atrophy and vision loss, which correlates with RGC loss [4, 5].

Optic neuritis has many causes; it may be associated to a broad range of autoimmune or infectious diseases [1, 6–9], and it is closely associated with multiple sclerosis (MS). In fact, ON is the initial symptom of MS in ~25% of cases, and may occur during the disease in about 70%, usually in the relapsing-remitting phase [1, 2]. On the other hand, acute ON often occurs as an isolated clinical event, without contributory systemic abnormalities, and it is retrospectively diagnosed as idiopathic (or primary) ON [1, 10].

Corticosteroids are the current mainstays of therapy for the treatment of ON. However, though steroids can be used to speed visual recovery, the overall visual improvement is unaffected by treatment [11]. In fact, corticosteroids do not prevent axonal loss or improve visual outcome [12, 13]. Therefore, a key area of therapeutic research is to identify neuroprotective drugs that can prevent axon and RGC loss, and hopefully lead to better visual outcomes.

Various rodent models representing different etiologies have been developed for ON studies. The most commonly used immune-mediated animal model for ON, is experimental autoimmune encephalomyelitis (EAE) [14], a

validated model for human MS [15, 16], which can be induced by active immunization with different myelin proteins or spontaneous transgenic models [16, 17]. However, the optic nerve lesions in EAE are associated with inflammation and demyelination of the brain and spinal cord, and, therefore, these models do not mimic the primary form of ON. Another type of ON model involves focal demyelination by using demyelinating toxins [18, 19]; however, these models lack the primary inflammatory component, which is pathognomonic of human primary ON. Recently, we have developed a new experimental model of primary ON in rats through a single microinjection of bacterial lipopolysaccharide (LPS) directly into the optic nerve [20]. The local injection of LPS induces a significant and persistent decrease in VEP amplitude and pupil light reflex (PLR), without changes in retinal function (electroretinogram). In addition, LPS induces a deficit in the anterograde transport from the retina to its central targets, and increased optic nerve microglial/macrophage reactivity, astrogliosis, demyelination, and axon and RGC loss, without signs of systemic inflammation or cerebral involvement [20]. These results suggest that the microinjection of LPS into the optic nerve may serve as a new experimental model of primary ON which could be useful for developing new therapeutic strategies.

Melatonin is involved in the regulation of many physiological functions, including the entrainment of seasonal and circadian rhythms. Moreover, melatonin has proven to be an antioxidant and anti-inflammatory molecule, able to reduce or mitigate cell damage associated with oxidative stress and inflammation processes that underlie neurodegenerative disorders (reviewed by [21–23]). In this line, experimental evidence strongly supports the actions of melatonin and its metabolites as a direct and indirect antioxidant [24–27], scavenging free radicals [24], stimulating antioxidant enzymes, and enhancing the activities of other antioxidants [28]. Moreover, the anti-inflammatory properties of melatonin have been accepted as a major protective mechanism on brain injury [29, 30]. In addition, several other mechanisms may be involved in neuroprotection induced by melatonin, like inhibition of the nitridergic pathway [31], and decreasing cyclooxygenase-2 (COX-2) activity [32], and vascular endothelial growth factor levels [33].

Besides the pineal gland, melatonin is also biosynthesized in the retina, where it behaves as an endogenous neuromodulator [34]. Melatonin may act as a protective agent in ocular conditions such as photo-keratitis, cataract, retinopathy of prematurity, and ischemia/reperfusion injury [35–37], as well as human refractory central serous chorioretinopathy [38]. Moreover, we have previously shown the beneficial effect of melatonin against retinal glaucomatous [39], uveitic [32, 40, 41], and type 2 diabetic [33] damage.

Since inflammatory response and oxidative stress play crucial roles in the progression of ON [42–44] the combination of immunomodulators and antioxidants is expected to improve the prognosis of ON [43]. In that context, the aim of the present report was to analyze the beneficial effect of melatonin on functional and histological alterations produced by experimental ON induced by the microinjection of LPS in the rat optic nerve.

## Materials and methods

### Animals

Male *Wistar* rats ( $300 \pm 50$  g) were housed in a standard animal room with food and water *ad libitum* under controlled conditions of temperature ( $21 \pm 2^\circ\text{C}$ ), luminosity (200 lux), and humidity, under a 12-hr light/12-hr dark lighting schedule (lights on at 8:00 AM). All animal procedures were in strict accordance with the Association for Research in Vision and Ophthalmology (ARVO) Statement for the Use of Animals in Ophthalmic and Vision Research. The ethic committee of the School of Medicine, University of Buenos Aires (Institutional Committee for the Care and Use of Laboratory Animals, (CICUAL)) approved this study, and all efforts were made to minimize animal suffering.

### Experimental model of ON

Animals were anesthetized with ketamine hydrochloride (150 mg/kg) and xylazine hydrochloride (2 mg/kg) administered intraperitoneally. Animal's head was shaved and the skin was disinfected with povidone-iodine (Pervinox). A lateral canthotomy was made to perform an incision of 2–3 mm. Lacrimal glands and extraocular muscles were dissected to expose 3 mm of the retrobulbar optic nerve under a surgical microscope. The optic nerve sheaths were opened longitudinally and a microinjection was performed with a 30G needle attached to a Hamilton syringe (Hamilton, Reno, NV, USA). The needle was inserted into the optic nerve as superficially as possible, 2 mm posterior to the globe, and 1  $\mu\text{L}$  of 4.5  $\mu\text{g}/\mu\text{L}$  *Salmonella typhimurium* LPS (Sigma Chemical Co., St Louis, MO, USA) in pyrogen-free saline, was injected for approximately 10 s. After injection, the skin incision was sutured and antibiotics were topically administered to prevent infection.

### Melatonin treatment

A group of rats was subcutaneously implanted with a pellet of melatonin (20 mg with 3% w/v vegetable oil) compressed in a bronze cylinder of 2.5 mm diameter and 1 mm length), while a control group was sham-operated without pellet implanting. The administration way and dose of melatonin were selected on the basis of previous reports [39, 41].

### Experimental design

In most of the experiments, vehicle was injected into one optic nerve and the contralateral optic nerve was injected with LPS. In these experiments, vehicle-injected optic nerves served as control because in a previous study, we found that vehicle injection per se did not affect optic nerve function and histology [20]. For the assessment of pupil light reflex (PLR), rats were injected with vehicle or LPS into one optic nerve, while the contralateral optic nerve remained intact. The pellet of 20 mg melatonin was implanted 1 day before vehicle or LPS injection, and was replaced every 10 days, and to analyze the therapeutic

effect of melatonin, a pellet of 20 mg melatonin was implanted at 4 days after vehicle and LPS injection, and was also replaced every 10 days. A total number of 156 rats were used for the experiments, distributed as follows: 38 rats in which one optic nerve was injected with vehicle and the contralateral optic nerve was injected with LPS in the absence of melatonin (eight animals for visual evoked potential (VEP) recording, five animals for anterograde transport study, five animals for immunohistochemical studies and luxol fast blue staining, five animals for semi-thin section analysis, five animals for lipid peroxidation measurement, five animals for Western blotting, and five animals for TNF $\alpha$  assessment); the same amount of rats was implanted with a pellet of 20 mg melatonin 24 hr before vehicle and LPS injections, and were equally distributed for each assay. In addition, eight rats in which one optic nerve was injected with vehicle or LPS and the contralateral optic nerve remained intact, and eight rats that were similarly treated but received a pellet of melatonin 24 hr before vehicle or LPS injections, were used for PLR assessment. Finally, to analyze the therapeutic effect of melatonin, eight animals in which one optic nerve was injected with vehicle and the contralateral optic nerve was injected with LPS in the absence of melatonin, and the same number of animals that were similarly treated but received a pellet of 20 mg melatonin at 4 days after vehicle and LPS injections were used for VEP recordings, and eight rats in which one optic nerve was injected with vehicle or LPS and the contralateral optic nerve remained intact, and eight rats that were similarly treated but received a pellet of 20 mg melatonin at 4 days after vehicle or LPS injections, were used for PLR assessment.

### Visual evoked potential recording

Animals were anesthetized as described above. Under stereotaxic control, two stainless steel electrodes, used as positive electrodes, were surgically placed 3 mm lateral to the inter-hemispheric suture and 5.6 mm behind bregma penetrating the cortex to approximately 0.5 mm. Reference electrodes were placed 2 mm lateral to the midline and 2 mm anterior to the bregma, as previously described [20]. The electrodes were isolated and covered with dental acrylic; skin was sutured with nylon 5/0, and antibiotics were administered topically.

After 5 days of electrode implantation, animals were dark adapted for 6 h, and anesthetized as described before. All recordings were made within 20 min after injection of anesthetic. The pupils were dilated with proparacaine (Alcon Midryl, Alcon Laboratories, Buenos Aires, Argentina), and the cornea was intermittently irrigated with saline solution. Each eye was individually recorded, occluding the contralateral eye with black carbon paper and cotton, and an average of 70 stimuli was recorded. Eyes were stimulated with unattenuated white light (1 Hz) by a photo stimulator with an intensity of 5 cds/m<sup>2</sup>, with filters for low and high frequency (0.5–100 Hz, respectively) and a 12.5 mV gain. The amplitude of N1-P2, and latency of P1, N1 and P2 components of VEPs were assessed with a software Akonic Bio-PC (Akonic, Buenos Aires, Argentina) coupled to a PC.

### Pupillary light reflex

Animals were injected with vehicle or LPS in one optic nerve while the contralateral optic nerve remained intact, and dark-adapted for 2 h. The eye in which the nerve was injected with vehicle or LPS was stimulated with high intensity light (1200 lux) for 30 s and the PLR was recorded in the contralateral (intact) eye. The recordings were made under infrared light with a digital video camera (Sony DCR-SR60, Tokyo, Japan), as previously described [45]. The sampling rate was 30 frames per second. Images were acquired with OSS Video Decompiler Software (One Stop Soft, New England, USA). The results were expressed as the percentage of the pupil contraction before (steady state) and 30 s after the light pulse.

### Cholera toxin $\beta$ -subunit transport studies

At 18 days postinjection of vehicle or LPS, rats were anesthetized, and a drop of 0.5% proparacaine (Anestalcon, Alcon Laboratories, Buenos Aires, Argentina) was topically administered for local anesthesia. Using a 30G Hamilton syringe (Hamilton, Reno, NV, USA), 4  $\mu$ L of 0.1% cholera toxin  $\beta$ -subunit (CTB) conjugated to Alexa 488 dye (Molecular Probes Inc., Eugene, OR, USA) in 0.1 mol/L PBS (pH 7.4) was injected into the vitreous, as previously described [46]. The injections were bilaterally applied 1 mm from the limbus, and the needle was left in the eye for 30 s to prevent volume loss. Three days after injection, rats were anesthetized and intracardially perfused. Brains were carefully removed, postfixed overnight at 4°C, and immersed in a graded series of sucrose solutions for cryoprotection; coronal sections (40  $\mu$ m) were obtained using a freezing microtome (CM 1850, Leica, Leica Microsystems, Buenos Aires, Argentina), mounted in glasses and viewed under an epifluorescence microscope (BX50, Olympus, Duarte, CA, USA). Every other coronal section was used for the SC retinorecipient area reconstruction, using Matlab (The Math-Works Inc., Natick, MA, USA). Digital images were converted to 8-bit grayscale, and the optic density of CTB staining was calculated. The total length was measured and divided into bins (4  $\mu$ m), from the medial to lateral region. CTB quantification was performed by dividing the total pixel area by CTB+ pixels. Finally, a colorimetric thermal representation was applied (from 0% = blue to 100% = red). The number of sections and the thickness (2X) were used for a final reconstruction of the retinal projection to the SC.

### Histological evaluation

Animals were deeply anesthetized and intracardially perfused with saline, followed by a fixative solution (4% paraformaldehyde in phosphate buffer (PBS), pH 7.2). Eye cups and optic nerves were obtained from the optic nerve head to the optic chiasm and postfixed in fixative solution for 24 hr at 4°C. After several washes, the samples were dehydrated, cleared in butanol and embedded in paraffin. Serial transversal sections (5  $\mu$ m) were obtained using a microtome (Leica, Leica Microsystems, Buenos Aires, Argentina). Some retinal sections were used for histological

analysis (hematoxylin-eosin (H&E) staining). Measurements (400 $\times$ ) were obtained at 1 mm dorsal and ventral from the optic disk. The average thickness (in  $\mu\text{m}$ ) of the total retina, inner plexiform layer (IPL), inner nuclear layer (INL), outer plexiform layer (OPL), outer nuclear layer (ONL), and photoreceptor outer segments (OS) were measured. For each sample, the average of four different sections was used as the representative value. After deparaffinization, some sections were hydrated and immersed overnight at 60°C in 0.1% luxol fast blue (Biopack, Buenos Aires, Argentina) in acidified 95% ethanol. Differentiation and counterstaining were carried out with 0.01%  $\text{Li}_2\text{CO}_3$  and incubation for 5 min in 0.5% neutral red (Biopack, Buenos Aires, Argentina). Sections were mounted and viewed under an optic microscope (Nikon Eclipse E400, Tokyo, Japan). Light microscopic images (200 $\times$ ) were digitally captured via a Nikon Coolpix S10 camera (Nikon, Tokyo, Japan).

### Semi-thin section processing

Anesthetized rats were intracardially perfused with saline solution, followed by a fixative solution containing 4% formaldehyde and 2% glutaraldehyde in 0.1 mol/L PBS (pH 7.4). Optic nerves were carefully removed, and portions (2 mm) near the eye were obtained and embedded in the same fixative solution for 24 hr. After several washings, some tissue blocks were postfixed in 2% aqueous osmium tetroxide in sodium phosphate buffer, for 1 hr. Dehydration was accomplished by gradual ethanol series, and tissue samples were embedded in epoxy resin. Semi-thin sections (0.5  $\mu\text{m}$ ) obtained with an ultramicrotome (Ultracut E, Reichert-Jung, Austria) were stained with toluidine blue, and used for morphometric analysis. Light microscopic images (200 $\times$  and 1000 $\times$ ) were digitally captured using a Nikon Eclipse E400 microscope via a Nikon Coolpix S10 camera (Nikon, Tokyo, Japan). Images obtained were assembled and processed using Adobe Photoshop CS5 (Adobe Systems, San Jose, CA, USA) to adjust brightness and contrast. Analysis image software (Image J, National Institutes of Health, Bethesda, Maryland, USA; <http://imagej.nih.gov/ij/>) were used to determinate axonal density.

### Immunohistochemical studies

Antigen retrieval was performed by heating slices at 90°C for 30 min in citrate buffer (pH 6.3). The following antibodies were used: a goat anti-ionized calcium binding adaptor molecule 1 (Iba-1) antibody (1:500; Abcam Inc., Buenos Aires, Argentina), a mouse anti-ED1 antibody (1:500; Abcam Inc., Buenos Aires, Argentina), a mouse monoclonal anti-gial fibrillary acidic protein (GFAP) antibody conjugated to Cy3 (1:1200; Sigma Chemical Co., St Louis, MO, USA), a donkey anti-mouse secondary antibody conjugated to Alexa 488 (1:500; Molecular Probes, Buenos Aires, Argentina), and a donkey anti-goat secondary antibodies conjugated to Alexa 568 (1:500; Molecular Probes, Buenos Aires, Argentina). Sections were immersed in 0.1% Triton X-100 in 0.1 mol/L PBS for 10 min, incubated with 2% normal horse serum for 1 hr for nonspecific blockade, and then incubated overnight

at 4°C with the primary antibodies. After several washings, secondary antibodies were added, and sections were incubated for 2 hr at room temperature. Regularly, some sections were treated without the primary antibodies to confirm specificity. For each nerve, results obtained from four separate regions were averaged, and the mean of 5 nerves was recorded as the representative value for each group. For immunodetection of RGCs, retinas were carefully detached and flat-mounted with the vitreous side up in superfrost microscope slides (Erie Scientific Company, Portsmouth, New Hampshire, USA). Whole-mount retinas were incubated overnight at 4°C with a goat anti-Brn3a antibody (1:500; Santa Cruz Biotechnology, Buenos Aires, Argentina). After several washes, a donkey anti-goat secondary antibody conjugated to Alexa 568 (1:500; Molecular Probes, Buenos Aires, Argentina) was added, and incubated for 2 hr at room temperature. Finally, retinas were mounted with fluorescent mounting medium, (Dako, Glostrup, Denmark), and observed under an epifluorescence microscope (BX50; Olympus, Tokyo, Japan) connected to a video camera (3CCD; Sony, Tokyo, Japan), attached to a computer running image analysis software (Image-Pro Plus; Media Cybernetics Inc., Bethesda, MD, USA). For each retina, results obtained from five separate quadrants were averaged, and the mean of 5 eyes was recorded as the representative value. Immunofluorescence studies were performed by analyzing comparative digital images from different samples by using identical exposure time, brightness, and contrast settings.

### Morphometric analysis

All the images obtained were assembled and processed using Adobe Photoshop CS5 (Adobe Systems, San Jose, CA, USA) to adjust brightness and contrast. No other adjustments were made. For all morphometric image processing and analysis, digitalized captured TIFF images were transferred to ImageJ software (National Institutes of Health, Bethesda, Maryland, USA; <http://imagej.nih.gov/ij/>).

### Measurement of thiobarbituric acid reactive substances (TBARS) levels

Two optic nerves were homogenized in 250  $\mu\text{L}$  of 15 mM potassium buffer plus 60 mM KCl, pH 7.2, and TBARS levels were analyzed as previously described [39]. The reaction mixture contained: optic nerve homogenate (100  $\mu\text{L}$ ), 25  $\mu\text{L}$  10% SDS, and 465  $\mu\text{L}$  0.8% thiobarbituric acid dissolved in 10% acetic acid (pH 3.5), and this solution was heated to 100°C for 60 min. After cooling, the precipitate was removed by centrifugation at 3200 g for 10 min. Then, 1.0 mL water and 5.0 mL of n-butanol-pyridine mixture (15:1, vol/vol) were added and the mixture was vigorously shaken and centrifuged at 2000 g for 15 min. The absorbance of the organic layer was measured at an emission wavelength of 553 nm by using an excitation wavelength of 515 nm with a Jasco FP 770 fluorescence spectrophotometer (Japan Spectroscopic Co. Ltd., Tokyo, Japan). The range of the standard curves of malondialdehyde bis-dimethyl acetal (MDA) was 10–2000 pmol.

Results were expressed as nanomol MDA/mg of wet tissue, and the intrassay coefficient of variation was lower than 8%.

### Western blotting

Optic nerves were homogenized in 250  $\mu$ L of a buffer containing 10 mM HEPES, 1 mM EDTA, 1 mM EGTA, 10 mM KCl, 0.5% (v/v) Triton, pH 7.9, supplemented with a cocktail of protease inhibitors (Sigma Chemical Co., St Louis, MO, USA). After 15 min at 4°C, homogenates were gently vortexed for 15 s and centrifuged at 900 g for 10 min at 4°C. Supernatants were used to determine protein concentration. Proteins (100  $\mu$ g/sample) were separated in SDS, 12% PAGE. After electrophoresis, proteins were transferred to polyvinylidene difluoride membranes for 60 min at 15-V in a Bio-Rad Trans-Blot S.D. system (Bio-Rad Laboratories, Hercules, CA, USA). Membranes were blocked in 3% BSA in Tris-buffered saline (pH 7.4) containing 0.1% Tween-20 for 60 min at room temperature and then incubated overnight at 4°C with a rabbit polyclonal anti-cyclooxygenase-2 (COX-2) antibody (1:200) and a rabbit polyclonal anti-inducible isoform of nitric oxide synthase (NOS-2) antibody (1:200). Membranes were washed and then incubated for 1 hr with a horseradish peroxidase-conjugated secondary antibody. Immunoblots were visualized by enhanced chemiluminescence Western blotting detection reagents (Amersham Biosciences, Buenos Aires, Argentina). Autoradiographical signals were quantified by densitometry using ImageQuant software and adjusted by the density of b-actin. For each group, the mean of 5 retinas were recorded as the representative value. Protein content was determined by the method of Lowry et al. [47], using BSA as the standard.

### Assay for TNF $\alpha$ level assessment

Optic nerves were homogenized in 150  $\mu$ L of phosphate saline buffer (PBS), pH 7.0, supplemented with 10% fetal bovine serum heat inactivated and a cocktail of protease

inhibitors. Samples were cleared by centrifugation for 10 min at 15 700 g. TNF $\alpha$  levels were determined as previously described [14], using specific rat enzyme-linked immunosorbent assays (ELISA) using antibodies and standards obtained from BD Biosciences, Pharmingen, San Diego, CA, USA, according to the manufacturer's instructions. The reaction was stopped and absorbance was read immediately at 450 nm on a microplate reader (Model 3550, BIO-RAD Laboratories, California, USA). The intrassay coefficient of variation was lower than 5%, and assay sensitivity was 0.5  $\mu$ g/mL.

### Protein level assessment

Protein content was determined by the method of Lowry et al. [47] using BSA as the standard.

### Statistical analysis

Data are presented as mean  $\pm$  standard error (SE). Statistical analysis of results was performed by two-way analysis of variance (ANOVA), followed by Tukey's test. *P* values below 0.05 were considered statistically significant.

## Results

To assess the effect of melatonin on the visual pathway dysfunction induced by experimental ON, flash VEPs were recorded at 21 days postinjection of vehicle or LPS into the optic nerve. Fig. 1 depicts the average VEP amplitude registered in animals untreated or treated with melatonin, in which one optic nerve was injected with vehicle, and the contralateral optic nerve was injected with LPS. LPS induced a significant decrease (72%, *P* < 0.05 versus control) in VEP N1-P2 component amplitude, which was completely (*P* < 0.01 versus LPS) prevented by melatonin. Representative waveforms of VEPs from all the experimental groups are also shown in Fig. 1. No significant differences in VEP amplitudes were evident in vehicle-injected optic nerves in the presence or absence of

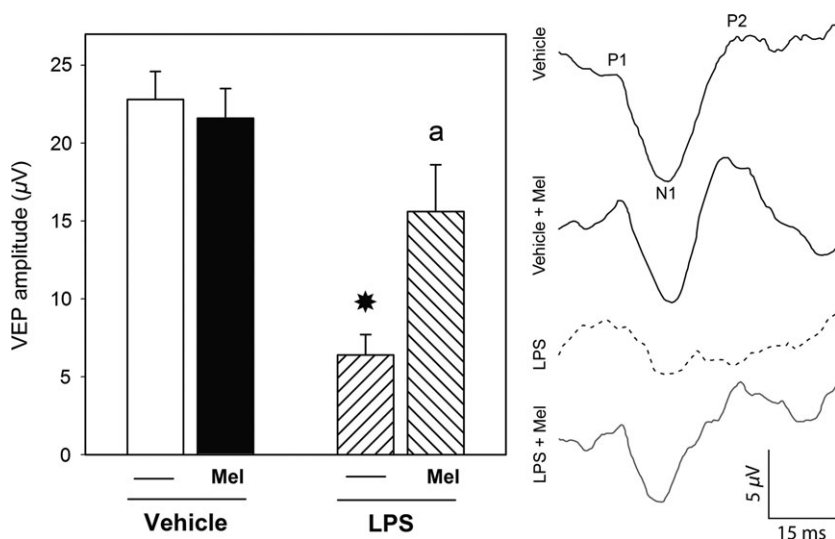


Fig. 1. Effect of LPS and melatonin on VEPs. Left panel: average amplitude of VEP N1-P2 component. Rat optic nerves were injected with vehicle or LPS in the presence or absence of a pellet of 20 mg melatonin, and VEPs were recorded at 21 days postinjection. Data are the mean  $\pm$  S.E.M. (n = 8 eyes/group). \**P* < 0.05 versus vehicle-injected optic nerves in the absence of melatonin, a: *P* < 0.01 versus LPS-injected optic nerves in the absence of melatonin, by Tukey's test. Right panel: representative VEP traces from all the experimental groups.

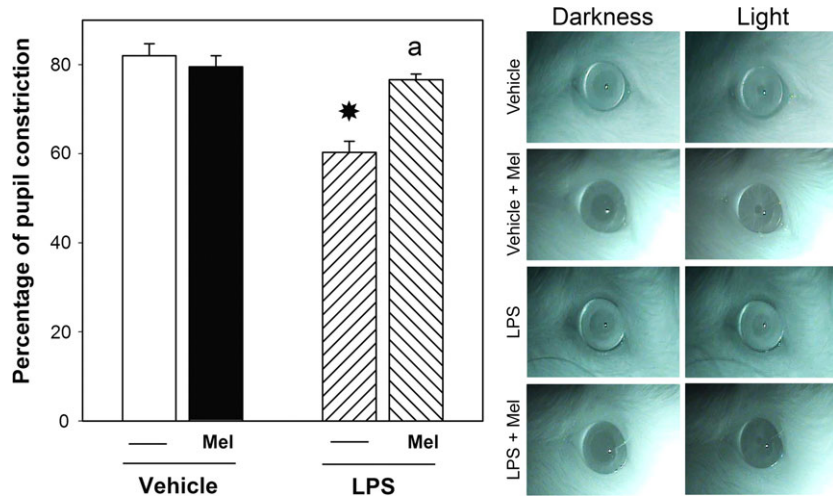


Fig. 2. Effect of LPS and melatonin on consensual PLR. Left panel: The rat pupil diameter (relative to the limbus diameter) was measured at 21 days postinjection of vehicle or LPS into the optic nerve, and the percentage of pupil constriction was calculated in the contralateral eye whose optic nerve remained intact. Data are the mean  $\pm$  S.E.M. ( $n = 8$  eyes/group). \* $P < 0.05$  versus vehicle-injected optic nerves in the absence of melatonin, a:  $P < 0.05$  versus LPS-injected optic nerves in the absence of melatonin, by Tukey's test. Right: Representative images of the consensual PLR in an animal in which one optic nerve was injected with vehicle or LPS in the absence or presence of a pellet of 20 mg melatonin.

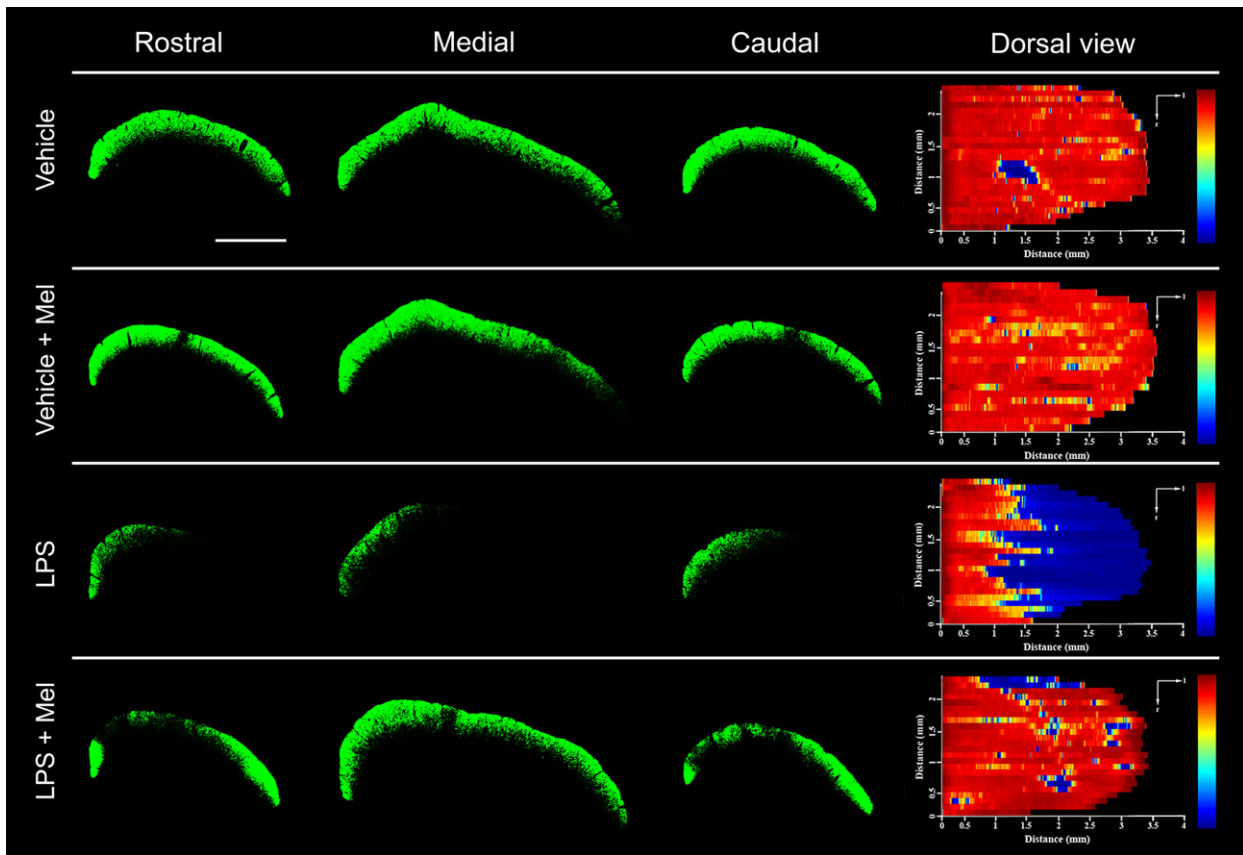


Fig. 3. Retinal projections in the SC. Left panel: Photomicrographs showing the CTB staining patterns in the retinotopic layers of the SC of rats injected with vehicle in one optic nerve and LPS in the contralateral optic nerve, in the absence or presence of melatonin. Three representative sections (rostral, medial, and caudal) are shown. A clear reduction in the density of retinal terminals and zones of no CTB staining were found in the SC contralateral to LPS-injected optic nerves, as compared with the SC contralateral to optic nerves injected with vehicle. A pellet of 20 mg melatonin preserved retinal anterograde transport through LPS-injected optic nerves. Shown are photomicrographs representative of five animals. Scale bar = 500  $\mu$ m. Right panel: Dorsal views of a retinotopic SC map reconstruction.

melatonin, and no differences in P1, N1, and P2 latencies were observed among groups (data not shown). To further analyze the effect of melatonin on the visual dysfunction induced by experimental ON, the PLR was examined in animals untreated or treated with melatonin in which one optic nerve was injected with vehicle or LPS, while in both cases, the contralateral optic nerve remained intact. When light stimulated eyes whose optic nerves were injected with LPS, a significant decrease (27%,  $P < 0.05$  versus control) in the pupil contraction of the contralateral intact eye was observed, whereas melatonin, which showed no effect per se, completely ( $P < 0.05$  versus LPS) prevented the effect of LPS on the PLR, as shown in Fig. 2.

The active anterograde transport from RGCs to the superior colliculus (SC) was analyzed using CTB intravitreally administered to animals in which one optic nerve was injected with vehicle and the contralateral optic nerve was injected with LPS. In the absence of melatonin, a reduction in CTB staining was observed in the entire retinotopic projection to the SC contralateral to optic nerves injected with LPS, whereas melatonin preserved CTB labeling in the SC. Melatonin did not affect retinal anterograde transport in the vehicle-treated optic nerve (Fig. 3).

Microglia/macrophages in the optic nerve were analyzed by Iba-1 and ED1 immunostaining, as shown in Fig. 4. A significant increase (~5 fold,  $P < 0.01$  versus control) in

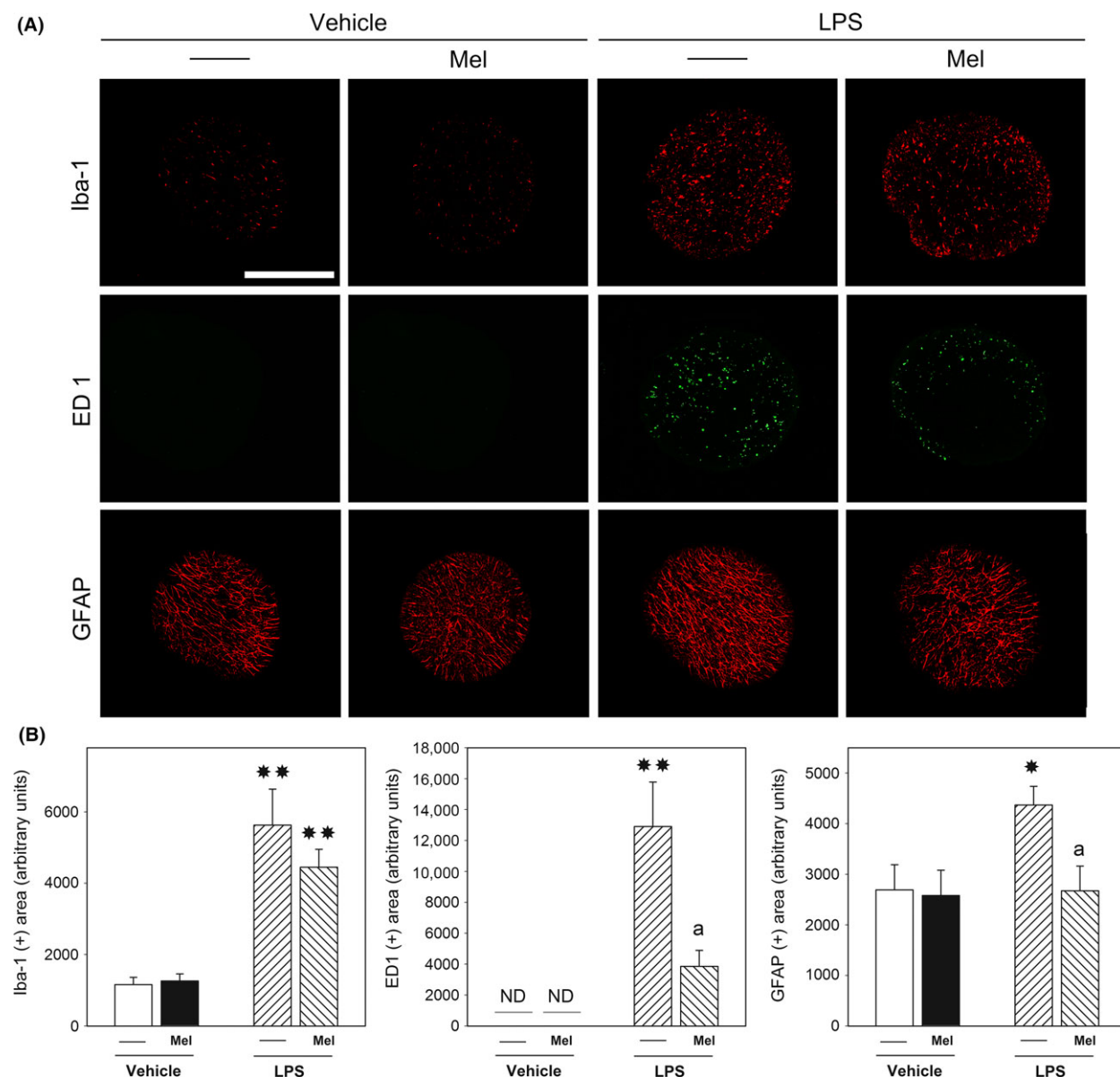


Fig. 4. Microglia/macrophage and astrocyte analysis in the rat optic nerve. Panel A: Representative photomicrographs showing Iba-1 (upper panel), ED1 (middle panel) and GFAP (lower panel) immunostaining in cross-sections from optic nerves at 21 days postinjection of vehicle or LPS in the presence or absence of a pellet of 20 mg melatonin. Scale bar = 200  $\mu$ m. Panel B: Analysis of Iba-1(+), ED1(+), and GFAP(+) area. Data are the mean  $\pm$  S.E.M. (n = 5 optic nerves per group); \* $P < 0.05$ , \*\* $P < 0.01$ , versus vehicle-injected optic nerves in the absence of melatonin, a:  $P < 0.05$  versus optic nerves injected with LPS in the absence of melatonin, by Tukey's test.

Iba-1(+) area in optic nerves was observed at 21 days postinjection of LPS. Melatonin did not affect the increase in Iba-1(+) area and significantly (64%,  $P < 0.01$  versus LPS) prevented the increase in ED1(+) area induced by LPS. In vehicle-injected optic nerves, no detectable ED1-immunoreactivity was found. To investigate astrocyte reactivity in vehicle- or LPS-injected optic nerves, GFAP-immunoreactivity in optic nerve cross-sections was examined. As shown in Fig. 4, a significant (162%,  $P < 0.05$  versus control) increase in GFAP(+) area was evident at 21 days postinjection of LPS, whereas in animals treated with melatonin, GFAP-immunoreactivity was similar to that observed in vehicle-injected optic nerves. Melatonin did not affect Iba-1-, ED1-, and GFAP-immunoreactivity in vehicle-injected optic nerves.

Demyelination was assessed by luxol fast blue staining. Signs of demyelination (50% of decrease in luxol fast blue staining,  $P < 0.05$  versus control) were evident at 21 days postinjection of LPS, whereas melatonin completely ( $P < 0.05$  versus LPS) prevented the occurrence of demyelination signs in LPS-injected optic nerves (Fig. 5). Optic nerve axons were analyzed by toluidine blue staining, as shown in Fig. 6. In the absence of melatonin, LPS induced a significant decrease (46%,  $P < 0.01$  versus control) in axon number, which was not evident in animals treated with melatonin ( $P < 0.01$  versus LPS). A morphometric analysis of retinal sections performed at 21 days postinjection of vehicle or LPS, revealed no differences in the total retina, IPL, INL, OPL, ONL, and OS layer thickness. To specifically examine RGCs, Brn3a-

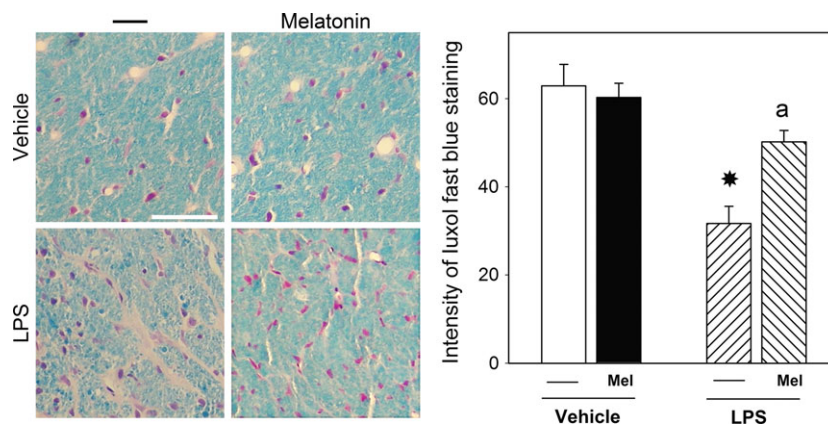


Fig. 5. Effect of LPS and melatonin on rat optic nerve myelination. Left panel: Representative cross-sections from optic nerves at 21 days postinjection of vehicle or LPS in the absence or presence of melatonin, stained with luxol fast blue. A compact myelin staining was observed in vehicle-injected optic nerves from animals untreated or treated with melatonin. Note a less stained area in LPS-injected optic nerve in the absence of melatonin, which was not evident in rats treated with a pellet of 20 mg melatonin. Scale bar = 50  $\mu$ m. Right panel: Evaluation of optic nerve demyelination by quantification of the staining intensity. LPS induced a significant demyelination of the optic nerve which was prevented by melatonin. Data are mean  $\pm$  S.E.M. (n: 5 optic nerves/group). \* $P < 0.05$  versus vehicle-injected optic nerves in the absence of melatonin, a:  $P < 0.05$  versus LPS-injected optic nerves in the absence of melatonin, by Tukey's test.

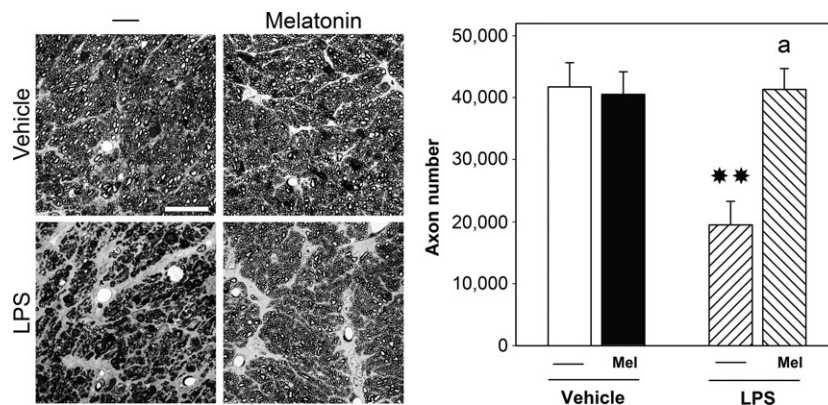
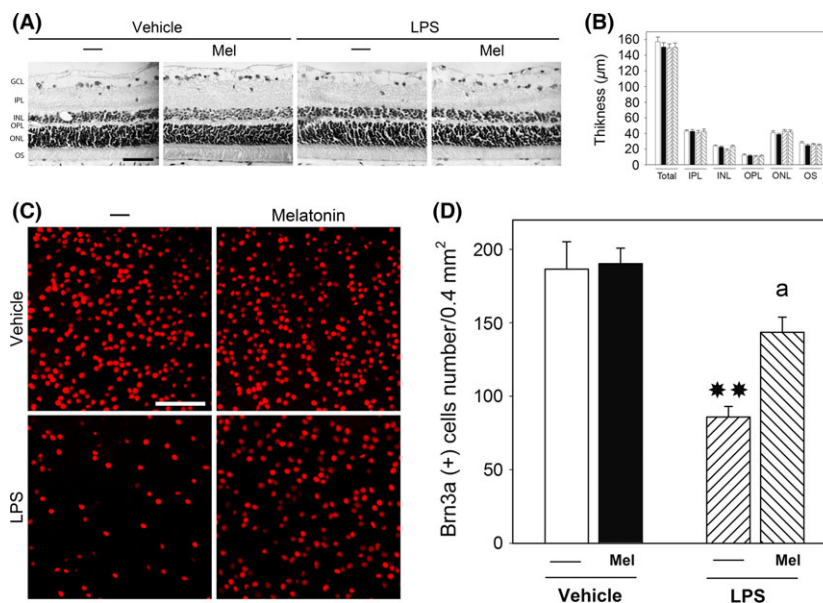


Fig. 6. Effect of LPS on optic nerve axons. Left panel: Representative images of cross-sections from vehicle- or LPS-injected optic nerves in the absence or presence of melatonin, stained with toluidine blue. Note the homogeneity of the staining in vehicle-injected optic nerves from rats untreated or treated with melatonin. In LPS-injected optic nerves, a less stained area was observed, which was not evident in LPS-injected optic nerves from animals treated with melatonin. Scale bar = 25  $\mu$ m. Right panel: The injection of LPS into the optic nerve induced a significant decrease in axon number, which was prevented by a pellet of 20 mg melatonin. Data are mean  $\pm$  S.E.M. (n: 5 optic nerves/group). \*\* $P < 0.01$  versus vehicle-injected optic nerves in the absence of melatonin, a:  $P < 0.01$  versus LPS-injected optic nerves in the absence of melatonin, by Tukey's test.



**Fig. 7.** Analysis of retinal structure and RGC number. Panel A: Representative photomicrographs of rat retinal sections from an eye whose optic nerve was injected with vehicle or LPS, in the presence or absence of melatonin. No evident alterations in retinal morphologic features were observed among group. Panel B: Total retinal and retinal layer thicknesses in all experimental groups. IPL, inner plexiform layer; INL, inner nuclear layer; OPL, outer plexiform layer; ONL, outer nuclear layer; OS, photoreceptor outer and inner segment. Panel C: Representative photomicrographs of Brn3a immunostaining in flatmounted retinas whose optic nerves were injected with vehicle or LPS in the absence or presence of a pellet of 20 mg melatonin. Panel D: Quantification of Brn3a(+) cells. Data are the mean  $\pm$  S.E.M. ( $n = 5$  retinas/group). \*\* $P < 0.01$  versus vehicle in the absence of melatonin, a:  $P < 0.01$  versus LPS in the absence of melatonin, by Tukey's test. Black scale bar = 50  $\mu\text{m}$ , white scale bar = 100  $\mu\text{m}$ .

immunostaining was analyzed in flatmounted retinas. A significant decrease in Brn3a(+) cell number (54%,  $P < 0.01$  versus control) was observed at 21 days postinjection of LPS, as shown in Fig. 7, which was completely ( $P < 0.01$  versus LPS) prevented by melatonin.

Figure 8 shows NOS-2, COX-2, and TNF $\alpha$  levels, as well as lipid peroxidation, in vehicle or LPS-injected optic nerve from animals untreated or treated with melatonin. The injection of LPS induced a significant increase in NOS-2 (260%,  $P < 0.01$  versus control), COX-2 (132%,  $P < 0.01$  versus control), and TNF $\alpha$  (176%,  $P < 0.01$  versus control) levels, and in lipid peroxidation (200%,  $P < 0.01$  versus control), whereas melatonin completely ( $P < 0.01$  versus LPS) prevented the increase in NOS-2, COX-2, and TNF $\alpha$  levels, and partly ( $P < 0.05$  versus control,  $P < 0.01$  versus LPS) prevented the increase in TBARS levels induced by LPS. When a pellet of 20 mg melatonin was implanted at 4 days after vehicle or LPS injection, a complete preservation ( $P < 0.01$  vs. LPS) of visual functions (VEPs and PLR) against damage induced by experimental ON was observed, as shown in Fig. 9.

## Discussion

For the first time, the present results indicate that melatonin provided visual function improvement in experimental ON, as shown by the preservation of VEPs and PLR. The functional protection was consistent with improved histopathologic outcomes (reduced microglial/macrophage reactivity, astrogliosis, demyelination, and axon and RGC loss), as well as with a decrease in inflammatory factors

(NOS-2, COX-2, and TNF $\alpha$ ) and oxidative damage. As previously shown [20], the consequences of LPS injection into the rat optic nerve can be apportioned to approximately two phases: an early phase (up to 7 days postinjection), characterized by functional (VEPs, PLR) alterations, and microglial/macrophage reactivity in the optic nerve, followed by a late phase (at 21 days postinjection), at which functional alterations and microglial/macrophage reactivity persist, and reactive gliosis, demyelination, and axon and RGC loss become evident. In this report, we chose to wait 21 days postinjection of LPS, in order to maximize functional and histological visual pathway damage, and to discard the possibility of a transient protection by melatonin. Moreover, we used pellets of 20 mg melatonin for reaching a continuous dosing to reduce the animal manipulation associated with a daily administration, and because in a previous report we showed the success of this dose and administration way for protecting the retina and optic nerve against damage induced by experimental glaucoma in rats [39]. In previous reports, we showed that melatonin prevents ocular inflammation in hamsters and cats with experimental uveitis [40, 41], and in dogs submitted to cataract surgery [37]. The present results further confirm the anti-inflammatory properties of melatonin in the visual pathway, in this case, by showing that melatonin was effective in preserving the optic nerve function and histology, as well as RGC number against damage induced by experimental ON. Glaucoma and ON are the two major degenerative causes of optic nerve damage [5], and a common feature of these optic neuropathies is RGC loss and axonal damage.

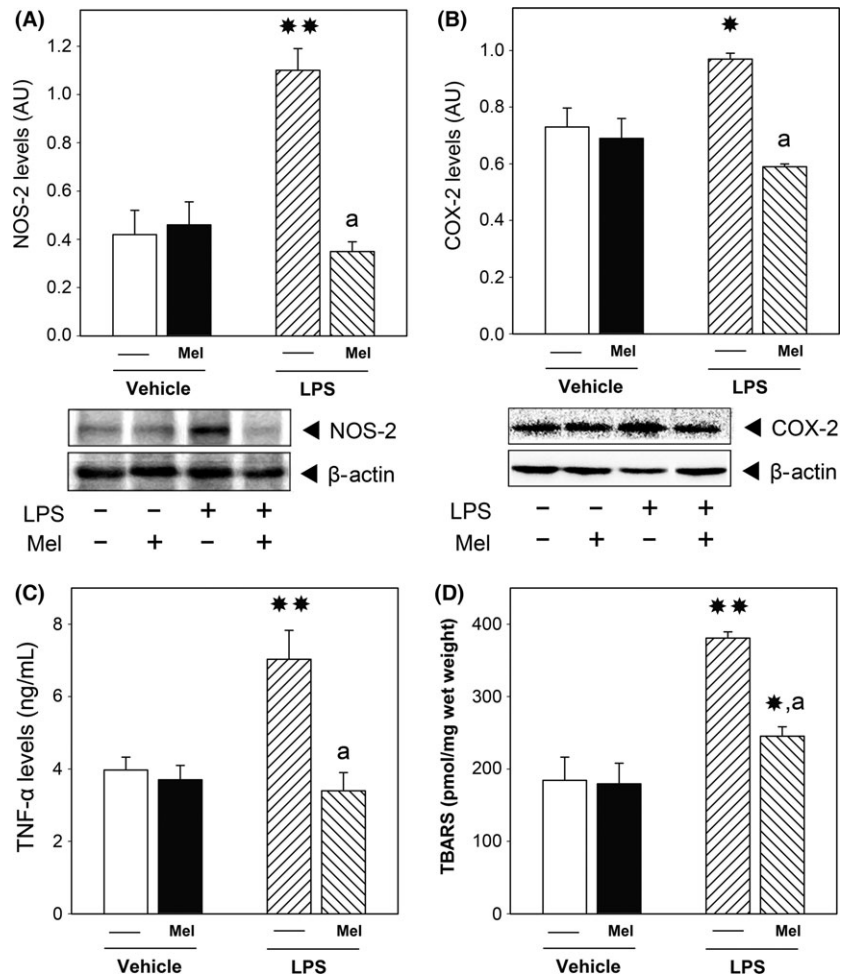


Fig. 8. Effect of LPS and melatonin on rat optic nerve NOS-2, COX-2, TNF $\alpha$ , and lipid peroxidation. NOS-2 (panel A), COX-2 (panel B), TNF $\alpha$  (panel C), and TBARs (panel D) levels. Representative Western blot analysis of NOS-2 and COX-2 level are shown in panel A and B respectively. Data are the mean  $\pm$  S.E.M. (n = 5 optic nerves/group). \* $P$  < 0.05, \*\* $P$  < 0.01 versus vehicle in the absence of melatonin, a:  $P$  < 0.01 versus LPS in the absence of melatonin, by Tukey's test.

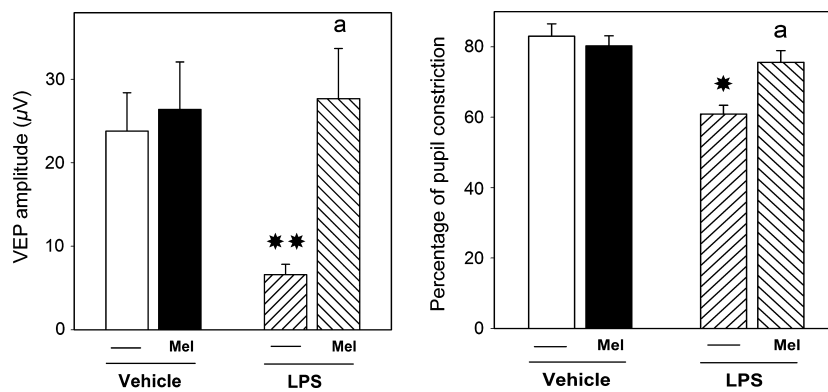


Fig. 9. Effect of a delayed treatment with melatonin on the visual pathway dysfunction induced by experimental ON in rats. At 4 days postinjection of vehicle or LPS into the optic nerve, a pellet of 20 mg melatonin was implanted subcutaneously, and VEP and PLR were assessed at 21 days postinjection. Left panel: average amplitude of VEP N1-P2 component. Right panel: Percentage of pupil constriction. Data are the mean  $\pm$  S.E.M. (n = 8 eyes/group). \* $P$  < 0.05, \*\* $P$  < 0.01 versus vehicle in the absence of melatonin, a:  $P$  < 0.01 versus LPS in the absence of melatonin, by Tukey's test.

Therefore, the present results are also consistent with the therapeutic effect of melatonin against experimental glaucomatous damage [39].

Visual evoked potential recording is considered an objective means of functional assessment of the integrity of the visual pathway [48]. In fact, VEP alteration is one

of the most characteristic electrophysiological signs observed in patients with ON, and remains as the preferred test for the detection of clinical and subclinical ON [49, 50]. Besides VEPs, pupillary testing is perhaps the most important bedside examination technique in suspected acute ON [51, 52]. As shown herein, melatonin

prevented the alterations in VEPs and PLR provoked by LPS-induced ON.

In rodents, most (~98%) RGC axons project contralaterally to the SC [53]. A defective axonal transport was described in mice with EAE-ON [54]. In agreement, LPS-induced ON provoked a “misconnection” between the retina and the SC, whereas melatonin prevented the deficit in the anterograde transport from the retina to its main synaptic target in rodents.

Microglial/macrophage activation is a key component of the inflammatory response. Increasing evidence indicates that an early inflammatory response contributes to the late stages of brain injury that result in neurological function loss [55], and it has been demonstrated that microglial activation and their progression towards a phagocytic state can lead to progressive and cumulative neuronal cell loss [56]. Iba-1 labels both quiescent and activated microglia/macrophage (providing an index of microglial/macrophage density), whereas abundance of the lysosomal antigen ED1 offers a measure of microglial phagocytic activity [57]. Although no changes in Iba-1(+) area were detected in LPS-injected optic nerves, melatonin decreased phagocytic microglial activation (as shown by a decrease in ED-1 immunoreactivity) induced by experimental ON. In agreement with these results, it has been demonstrated that melatonin restrains the activation of microglia following traumatic brain injury [29], and attenuates LPS-induced increase in microglial reactivity in the neonatal rat brain [58]. Besides microglia, it has been shown that astrocyte responses contribute to EAE-ON pathology [59]. In this line, melatonin significantly prevented the reactive gliosis (assessed by GFAP-immunoreactivity) in LPS-injected optic nerves.

Melatonin has a potent protective effect on white matter, enhancing oligodendroglial maturation and myelination [60]. In agreement, melatonin prevented the occurrence of demyelination signs (as shown by luxol fast blue staining) in the optic nerve induced by LPS injection. Although we could not ascertain whether the protection induced by melatonin primarily occurred in axons or glial elements, our results could suggest that alterations in the bidirectional communication between axons and glial cells induced by experimental ON can be positively affected by melatonin. In addition, since axonal damage often results in axonal degeneration and permanent loss of the cell body, the preservation of RGC number is consistent with the prevention of axon loss induced by melatonin.

There remain to be established the mechanism/s involved in the therapeutic benefit of melatonin in experimental ON. Improper upregulation of inflammatory signals such as TNF $\alpha$ , COX-2, and NOS-2 has been associated with the pathophysiology of EAE-ON [61]. Moreover, oxidative stress is known to induce neuronal damage in experimental ON [44]. As shown herein, melatonin prevented the increase in NOS-2, COX-2, and TNF- $\alpha$  levels, which could be consistent with the reduced microglial activation, and optic nerve lipid peroxidation, which is consistent with its well-known antioxidant activity. Thus, it seems likely that melatonin may attenuate the severity of experimental ON by exerting anti-inflammatory and antioxidant effects. Established strategies for the

treatment of EAE-ON mainly target the autoimmune response by using anti-inflammatory, immunomodulatory, and immunosuppressive agents, but none of them have clear neuroprotective properties [62]. In fact, corticoid pulse therapy as the standard treatment for human ON can only promote the recovery of visual acuity, but does not prevent RGC degeneration and does not improve ultimate visual outcome [11–13]. Since a significant RGC loss seems to be the main cause of permanent visual function damage in both experimental models of ON and patients with ON, an optimal therapeutic strategy may require a combination of a immunosuppressive and anti-inflammatory treatment combined with a neuroprotective agent [43]. The present results support that melatonin could be able to fulfill these requirements, since it suppressed visual impairment, prevented optic nerve structural alterations and RGC loss, and decreased inflammatory signals and oxidative stress induced by experimental ON. Despite the preventive effect of melatonin in LPS-induced ON, the translational relevance of these results is limited by the fact that melatonin was administered before LPS injection. Therefore, the following experiments were performed to analyze whether melatonin also preserves visual function when the treatment is initiated after the onset of ON. It is important to emphasize the fact that a significant decrease in VEP amplitude and PLR is already evident at 1 day postinjection of LPS and persists for at least 21 days postinjection [20]. As shown herein, a delayed treatment with melatonin (administered at 4 days postinjection of LPS) significantly reduced the visual dysfunction (VEP and PLR) induced by experimental ON, supporting that melatonin not only prevented, but also reduced the progression of optic nerve damage. Overall, the current study demonstrates an ability of melatonin to significantly preserve visual functions in experimental ON, with reduction of inflammation, astrocytosis, demyelination, and axon and RGC loss. These neuroprotective effects may involve anti-inflammatory and/or antioxidant effects; and by either mechanism, melatonin, a very safe compound (even at high doses) for human use, could represent a promising potential therapy for primary ON.

## Acknowledgments

This research was supported by grants from the Agencia Nacional de Promoción Científica y Tecnológica [PICT 0610]; The University of Buenos Aires [20020100100678]; Consejo Nacional de Investigaciones Científicas y Técnicas [PIP 1911], Argentina. The funding organizations have no role in the design or conduct of this research. The authors report no conflicts of interest.

## Author Contributions

Marcos L. Aranda: contributions to concept/design, acquisition of data, data analysis/interpretation. María F. González Fleitas: acquisition of data. Andrea De Laurentiis: acquisition of data. María I. Keller Sarmiento: acquisition of data. Mónica Chianelli: acquisition of data. Pablo H. Sande: contributions to concept/design, acquisition of data. Damian Dorfman: contributions to

concept/design, data analysis/interpretation, and approval of the article. Ruth E. Rosenstein: contributions to concept/design, data analysis/interpretation, drafting of the manuscript, and approval of the article.

## References

- HICKMAN SJ, DALTON CM, MILLER DH et al. Management of acute optic neuritis. *Lancet* 2002; **360**:1953–1962.
- TOOSY AT, MASON DF, MILLER DH. Optic neuritis. *Lancet Neurol* 2014; **13**:83–99.
- MARTÍNEZ-LAPISCINA EH, FRAGA-PUMAR E, PASTOR X et al. Is the incidence of optic neuritis rising? Evidence from an epidemiological study in Barcelona (Spain), 2008–2012. *J Neurol* 2014; **261**:759–767.
- TRIP SA, SCHLOTTMANN PG, JONES SJ et al. Retinal nerve fiber layer axonal loss and visual dysfunction in optic neuritis. *Ann Neurol* 2005; **58**:383–391.
- YOU Y, GUPTA VK, LI JC et al. Optic neuropathies: characteristic features and mechanisms of retinal ganglion cell loss. *Rev Neurosci* 2013; **24**:301–321.
- EGGENBERGER ER. Inflammatory optic neuropathies. *Ophthalmol Clin North Am* 2001; **14**:73–82.
- FRIGUI M, FRIKHA F, SELLEMI D et al. Optic neuropathy as a presenting feature of systemic lupus erythematosus: two case reports and literature review. *Lupus* 2011; **20**:1214–1218.
- HORWITZ H, FRIIS T, MODVIG S et al. Differential diagnoses to MS: experiences from an optic neuritis clinic. *J Neurol* 2014; **261**:98–105.
- KALLENBACH K, FREDERIKSEN JL. Unilateral optic neuritis as the presenting symptom of human immunodeficiency virus toxoplasmosis infection. *Acta Ophthalmol* 2008; **86**:459–460.
- Optic Neuritis Study Group. Multiple sclerosis risk after optic neuritis: final optic neuritis treatment trial follow-up. *Arch Neurol* 2008; **65**:727–732.
- BECK RW, GAL RL. Treatment of acute optic neuritis: a summary of findings from the optic neuritis treatment trial. *Arch Ophthalmol* 2008; **126**:994–995.
- GAL RL, VEDULA SS, BECK R. Corticosteroids for treating optic neuritis. *Cochrane Database Syst Rev* 2015; **8**:CD001430.
- HICKMAN SJ, KAPOOR R, JONES SJ et al. Corticosteroids do not prevent optic nerve atrophy following optic neuritis. *J Neurol Neurosurg Psychiatry* 2003; **74**:1139–1141.
- WEKERLE H, KOJIMA K, LANNES-VIEIRA J et al. Animal models. *Ann Neurol* 1994; **36**(Suppl):S47–S53.
- GOLD R, LININGTON C, LASSMANN H. Understanding pathogenesis and therapy of multiple sclerosis via animal models: 70 years of merits and culprits in experimental autoimmune encephalomyelitis research. *Brain* 2006; **129**:1953–1971.
- ROBINSON AP, HARP CT, NORONHA A et al. The experimental autoimmune encephalomyelitis (EAE) model of MS: utility for understanding disease pathophysiology and treatment. *Handb Clin Neurol* 2014; **122**:173–189.
- GUPTA AA, DING D, LEE RK et al. Spontaneous ocular and neurologic deficits in transgenic mouse models of multiple sclerosis and noninvasive investigative modalities: a review. *Invest Ophthalmol Vis Sci* 2012; **53**:712–724.
- LACHAPPELLE F, BACHELIN C, MOISSONNIER P et al. Failure of remyelination in the nonhuman primate optic nerve. *Brain Pathol* 2005; **15**:198–207.
- YOU Y, KLITORNER A, THIE J et al. Latency delay of visual evoked potential is a real measurement of demyelination in a rat model of optic neuritis. *Invest Ophthalmol Vis Sci* 2011; **52**:6911–6918.
- ARANDA ML, DORFMAN D, SANDE PH et al. Experimental optic neuritis induced by the microinjection of lipopolysaccharide into the optic nerve. *Exp Neurol* 2015; **266**:30–41.
- ESCRIBANO BM, COLÍN-GONZÁLEZ AL, SANTAMARÍA A et al. The role of melatonin in multiple sclerosis, Huntington's disease and cerebral ischemia. *CNS Neurol Disord Drug Targets* 2014; **13**:1096–1119.
- MAURIZ JL, COLLADO PS, VENEROSO C et al. A review of the molecular aspects of melatonin's anti-inflammatory actions: recent insight and new perspectives. *J Pineal Res* 2013; **54**:1–14.
- GARCIA JJ, LOPEZ-PINGARRON L, ALMEIDA-SOUZA P et al. Protective effects of melatonin in reducing oxidative stress and in preserving the fluidity of biological membranes: a review. *J Pineal Res* 2014; **56**:225–237.
- GALANO A, TAN DX, REITER RJ. On the free radical scavenging activities of melatonin's metabolites, AFMK and AMK. *J Pineal Res* 2013; **54**:245–257.
- REITER RJ, PAREDES SD, MANCHESTER LC et al. Reducing oxidative/nitrosative stress: a newly-discovered genre for melatonin. *Crit Rev Biochem Mol Biol* 2009; **44**:175–200.
- ZHANG HM, ZHANG Y. Melatonin: a well-documented antioxidant with conditional pro-oxidant actions. *J Pineal Res* 2014; **57**:131–146.
- MANCHESTER LC, COTO-MONTES A, BOGA JA et al. Melatonin: an ancient molecule that makes oxygen metabolically tolerable. *J Pineal Res* 2015; **59**:403–419.
- RODRIGUEZ C, MAYO JC, SAINZ RM et al. Regulation of antioxidant enzymes: a significant role for melatonin. *J Pineal Res* 2004; **36**:1–9.
- DING K, WANG H, XU J et al. Melatonin reduced microglial activation and alleviated neuroinflammation induced neuron degeneration in experimental traumatic brain injury: possible involvement of mTOR pathway. *Neurochem Int* 2014; **76**:23–31.
- SAMANTARAY S, DAS A, THAKORE NP et al. Therapeutic potential of melatonin in traumatic central nervous system injury. *J Pineal Res* 2009; **47**:134–142.
- SAENZ DA, TURJANSKI AG, SACCA GB et al. Physiological concentrations of melatonin inhibit the nitridergic pathway in the Syrian hamster retina. *J Pineal Res* 2002; **33**:31–36.
- SANDE PH, DORFMAN D, FERNANDEZ DC et al. Treatment with melatonin after onset of experimental uveitis attenuates ocular inflammation. *Br J Pharmacol* 2014; **171**:5696–5707.
- SALIDO EM, BORDONE M, de LAURENTIIS A et al. Therapeutic efficacy of melatonin in reducing retinal damage in an experimental model of early type 2 diabetes in rats. *J Pineal Res* 2013; **54**:179–189.
- ROSENSTEIN RE, PANDI-PERUMAL SR, SRINIVASAN V et al. Melatonin as a therapeutic tool in ophthalmology: implications for glaucoma and uveitis. *J Pineal Res* 2010; **49**:1–13.
- ALIO JL, AYALA MJ, MULET E et al. Treatment of experimental acute corneal inflammation with inhibitors of the oxidative metabolism. *Ophthalmic Res* 1993; **25**:331–336.
- SIU AW, MALDONADO M, SANCHEZ-HIDALGO M et al. Protective effects of melatonin in experimental free radical-related ocular diseases. *J Pineal Res* 2006; **40**:101–109.
- SANDE PH, ÁLVAREZ J, CALCAGNO J et al. Preliminary findings on the effect of melatonin on the clinical outcome of cataract surgery in dogs. *Vet Ophthalmol* 2015; doi:10.1111/vop.12282.

38. GRAMAJO AL, MARQUEZ GE, TORRES VE et al. Therapeutic benefit of melatonin in refractory central serous chorioretinopathy. *Eye (Lond)* 2015; **29**:1036–1045.
39. BELFORTE NA, MORENO MC, de ZAVALÍA N et al. Melatonin: a novel neuroprotectant for the treatment of glaucoma. *J Pineal Res* 2010; **48**:353–364.
40. del SOLE MJ, SANDE PH, FERNANDEZ DC et al. Therapeutic benefit of melatonin in experimental feline uveitis. *J Pineal Res* 2012; **52**:29–37.
41. SANDE PH, FERNANDEZ DC, ALDANA MARCOS HJ et al. Therapeutic effect of melatonin in experimental uveitis. *Am J Pathol* 2008; **173**:1702–1713.
42. CHAUDHARY P, MARRACCI G, YU X et al. Lipoic acid decreases inflammation and confers neuroprotection in experimental autoimmune optic neuritis. *J Neuroimmunol* 2011; **233**:90–96.
43. LI K, DU Y, FAN Q et al. Gypenosides might have neuroprotective and immunomodulatory effects on optic neuritis. *Med Hypotheses* 2014; **82**:636–638.
44. Qi X, LEWIN AS, SUN L et al. Suppression of mitochondrial oxidative stress provides long-term neuroprotection in experimental optic neuritis. *Invest Ophthalmol Vis Sci* 2007; **48**:681–691.
45. FERNANDEZ DC, SANDE PH, de ZAVALÍA N et al. Effect of experimental diabetic retinopathy on the non-image-forming visual system. *Chronobiol Int* 2013; **30**:583–597.
46. DORFMAN D, FERNANDEZ DC, CHIANELLI M et al. Post-ischemic environmental enrichment protects the retina from ischemic damage in adult rats. *Exp Neurol* 2013; **240**:146–156.
47. LOWRY OH, ROSEBROUGH NJ, FARR AL et al. Protein measurement with the Folin phenol reagent. *J Biol Chem* 1951; **193**:265–275.
48. HALLIDAY A, McDONALD W, MUSHIN J. Delayed visual evoked response in optic neuritis. *Lancet* 1972; **1**:982–985.
49. NAISMITH RT, TUTLAM NT, XU J et al. Optical coherence tomography is less sensitive than visual evoked potentials in optic neuritis. *Neurology* 2009; **73**:46–52.
50. SHANDIZ JH, NOURIAN A, HOSSAINI MB et al. Contrast sensitivity versus visual evoked potentials in multiple sclerosis. *J Ophthalmic Vis Res* 2010; **5**:175–181.
51. de SEZE J, ARNDT C, STOJKOVIC T et al. Pupillary disturbances in multiple sclerosis: correlation with MRI findings. *J Neurol Sci* 2001; **188**:37–41.
52. MORO SI, RODRIGUEZ-CARMONA ML, FROST EC et al. Recovery of vision and pupil responses in optic neuritis and multiple sclerosis. *Ophthalmic Physiol Opt* 2007; **27**:451–460.
53. KONDO Y, TAKADA M, HONDA Y et al. Bilateral projections of single retinal ganglion cells to the lateral geniculate nuclei and superior colliculi in the albino rat. *Brain Res* 1993; **608**:204–215.
54. LIN TH, KIM JH, PEREZ-TORRES C et al. Axonal transport rate decreased at the onset of optic neuritis in EAE mice. *NeuroImage* 2014; **100**:244–253.
55. KAUSHIK DK, BASU A. A friend in need may not be a friend indeed: role of microglia in neurodegenerative diseases. *CNS Neurol Disord Drug Targets* 2013; **12**:726–740.
56. NEHER JJ, EMMRICH JV, FRICKER M et al. Phagocytosis executes delayed neuronal death after focal brain ischemia. *Proc Natl Acad Sci USA* 2013; **110**:E4098–E4107.
57. EBNETER A, CASSON RJ, WOOD JP et al. Microglial activation in the visual pathway in experimental glaucoma: spatiotemporal characterization and correlation with axonal injury. *Invest Ophthalmol Vis Sci* 2010; **51**:6448–6460.
58. WONG CS, JOW GM, KAIZAKI A et al. Melatonin ameliorates brain injury induced by systemic lipopolysaccharide in neonatal rats. *Neuroscience* 2014; **267**:147–156.
59. BRAMBILLA R, DVORIANCHIKOVA G, BARAKAT D et al. Transgenic inhibition of astroglial NF- $\kappa$ B protects from optic nerve damage and retinal ganglion cell loss in experimental optic neuritis. *J Neuroinflammation* 2012; **9**:213.
60. ESPOSITO E, CUZZOCREA S. Antiinflammatory activity of melatonin in central nervous system. *Curr Neuropharmacol* 2010; **8**:228–242.
61. DAS A, GUYTON MK, SMITH A et al. Calpain inhibitor attenuated optic nerve damage in acute optic neuritis in rats. *J Neurochem* 2013; **124**:133–146.
62. DIEM R, HOBOM M, MAIER K et al. Methylprednisolone increases neuronal apoptosis during autoimmune CNS inflammation by inhibition of an endogenous neuroprotective pathway. *J Neurosci* 2003; **23**:6993–7000.